

Eudialyte-group minerals from the Monte de Trigo alkaline suite, Brazil: composition and petrological implications

Minerais do grupo da eudialita da suíte alcalina Monte de Trigo, Brasil: composição e implicações petrológicas

Gaston Eduardo Enrich Rojas^{1*}, Excelso Ruberti¹,
Rogério Guitarrari Azzone¹, Celso de Barros Gomes¹

ABSTRACT: The Monte de Trigo alkaline suite is a SiO_2 -undersaturated syenite-gabbroid association from the Serra do Mar alkaline province. Eudialyte-group minerals (EGMs) occur in one nepheline microsyenite dyke, associated with aegirine-augite, wöhlertite, lavenite, magnetite, zircon, titanite, britholite, and pyrochlore. Major compositional variations include Si (25.09–25.57 apfu), Nb (0.31–0.76 apfu), Fe (1.40–2.13 apfu), and Mn (1.36–2.08 apfu). The EGMs also contain relatively high contents of Ca (6.13–7.10 apfu), moderate enrichment of rare earth elements (0.38–0.67 apfu), and a relatively low Na content (11.02–12.28 apfu), which can be correlated with their transitional agpaitic assemblage. EGM compositions indicate a complex solid solution that includes eudialyte, kentbrooksite, feklichevite, zirsilite-(Ce), georgbarsanovite, and manganeseeudialyte components. EGM trace element analyses show low Sr and Ba contents and a negative Eu/Eu* anomaly, which are interpreted as characteristic of the parental magma due to the previous fractionation of plagioclase and/or alkali feldspar. The EGMs from the dyke border have higher contents of Fe, Sr (2,161–2,699 ppm), Mg (1,179–3,582 ppm), and Zn (732–852 ppm) than those at the dyke center. These differences are related to the incorporation of xenoliths and xenocrysts of melatheralitic host rock into the nepheline-syenitic magma followed by crystal-melt diffusive exchange.

KEYWORDS: mineral chemistry; agpaitic rocks; Serra do Mar alkaline province.

RESUMO: A suíte alcalina do Monte de Trigo é uma associação sienítico-gabroide que pertence à província alcalina da Serra do Mar. Minerais do grupo da eudialita (EGMs) ocorrem em um dique de nefelina microssienito associados a egirina-augita, wöhlerita, lavenita, magnetita, zircão, titanita, britolita e pirocloro. As principais variações composticionais incluem Si (25,09–25,57 apfu), Nb (0,31–0,76 apfu), Fe (1,40–2,13 apfu) e Mn (1,36–2,08 apfu). Os EGMs também contêm concentrações relativamente altas de Ca (6,13–7,10 apfu), enriquecimento moderado de elementos terras raras (0,38–0,67 apfu) e concentrações relativamente baixas de Na (11,02–12,28 apfu), o que pode ser correlacionado com uma assembleia agpaitica transicional. As composições dos EGMs indicam uma solução sólida complexa entre os componentes eudialita, kentbrooksite, feklichevite, zirsilita-(Ce), georgbarsanovita e manganoeudialita. Análises de elementos traços das EGMs mostram baixas concentrações de Sr e Ba e anomalia negativa de Eu/Eu*, que são interpretadas como uma característica do magma parental por conta do fracionamento de plagioclásio e/ou feldspato alcalino. Os EGMs da borda do dique possuem concentrações maiores de Fe, Sr (2,161–2,699 ppm), Mg (1,179–3,582 ppm) e Zn (732–852 ppm) que aqueles do centro do dique. Essas diferenças estão relacionadas com a incorporação de xenólitos e xenocristais da rocha encaixante melateralítica no magma nefelina-sienítico seguido de trocas difusivas entre os cristais e o líquido.

PALAVRAS-CHAVE: química mineral; rochas agpaiticas, província alcalina da Serra do Mar.

¹Instituto de Geociências, University of São Paulo - USP, São Paulo (SP), Brasil. E-mail: gastonenrich@usp.br, exrubert@usp.br, rgazzone@usp.br, cgomes@usp.br

*Autor correspondente

Manuscript: 20160075. Received on: 06/13/2016. Approved on: 08/09/2016

INTRODUCTION

The eudialyte group minerals (EGMs) consist of various Na-, Ca-, and Zr-rich cyclosilicates with a wide compositional variation. Significant amounts of other elements, such as Fe, Mn, Nb, rare earth elements (REE), Sr, and Cl are reported in EGM compositions (Johnsen & Gault 1997, Johnsen & Grice 1999, Schilling et al. 2011b). According to the International Mineralogical Association (Johnsen et al. 2003), the general formula of the EGMs is $\text{Na}_{12}[\text{N}(4)]_3[\text{M}(1)]_6[\text{M}(2)]_3[\text{M}(3)][\text{M}(4)]\text{Zr}_3(\text{Si}_{24}\text{O}_{72})$ ($\text{O}, \text{OH}, \text{H}_2\text{O}$)₄ X_2 , in which the common elements assigned to each site are as it follows:

- Si at $M(4)$;
- Nb, Si, Ti, and W at $M(3)$;
- Fe, Mn, Na, Zr, K, and H_3O at $M(2)$;
- Ca, Mn, and Fe at $M(1)$;
- Na, REE, Sr, K, Ca, Mn, and H_3O at $N(4)$;
- Cl, OH, F, and CO_3 at X .

Rastsvetaeva & Chukanov (2012) list 25 known species of EGMs, and recently a new member named Ilyukhinite was described (Chukanov et al. 2015). This great diversity is the result of the compositional and structural complexity of the group.

Eudialyte was first described by Stromeyer (1819) as one of the major constituents of nepheline syenites from the Ilímaussaq Complex, Greenland. Since then, EGMs have been recognized in nearly all occurrences of agpaitic rocks, i.e., peralkaline nepheline syenites (and phonolites) that contain complex silicates of Zr, Ti, REE, F, and other volatiles (Sørensen 1997, Le Maitre 2002). EGMs have been described in agpaitic rocks from Khibiny and Lovozero, Kola Peninsula (Khomyakov 1995, Johnsen & Gault 1997, Schilling et al. 2011b); Mont Saint-Hilaire, Canada (Johnsen & Gault 1997, Johnsen & Grice 1999, Schilling et al. 2011b); Langesundsfjord, Norway (Andersen et al. 2010, Schilling et al. 2011b); Tamazeght, Morocco (Schilling et al. 2009, Schilling et al. 2011b); Poços de Caldas, Brazil (Johnsen & Gault 1997, Ulbrich & Ulbrich 2000, Ulbrich et al. 2005, Schilling et al. 2011b); Cerro Boggiani, Paraguay (Gomes et al. 1996, Carbonin et al. 2005); Pilanesberg, South Africa (Mitchell & Liferovich, 2006, Schilling et al. 2011a); Sushina Hill, India (Mitchell & Chakrabarty, 2012); Agua de Pau volcano, Azores, Portugal (Ridolfi et al. 2003); and Kilombe volcano, Kenya Rift Valley (Ridolfi et al. 2006). The typical minerals associated with EGMs include alkali feldspar, nepheline, sodalite, aegirine, arfvedsonite, and several complex Zr-, Nb-, Ti-, and REE-bearing silicates, such as astrophyllite, lamprophyllite, rosenbuschite, rinkite, and wöhlerite (e.g.,

Sørensen 1997, Andersen et al. 2010, Marks et al. 2011, Schilling et al. 2011b).

The present paper reports the occurrence of EGMs from the alkaline suite of Monte de Trigo, a small island (ca. 1 km²) situated near the towns of São Paulo and Rio de Janeiro, at the western border of the Santos Basin (23°53'S, 45°47'W), in southeastern Brazil. They describes major and trace element analyses of these EGMs, and their composition is discussed in terms of site assignment and possible ideal components. The objectives of the study were to characterize the EGMs at Monte de Trigo and to understand how its petrological environment influences the major and trace element compositions of the EGMs.

MAGMATIC CONTEXT

Several late cretaceous alkaline occurrences and widespread lamprophyre dyke swarms intrude the Neoproterozoic Ribeira belt in southeastern Brazil and constitute the Serra do Mar Alkaline Province (Fig. 1A; Almeida 1983, Thompson et al. 1998, Riccomini et al. 2005, Brotzu et al. 2005). This province is part of an extensive Meso-Cenozoic tholeiitic–alkaline–carbonatic magmatism that is spread over the central and southeastern regions of the Brazilian Platform (Morbidelli et al. 1995, Peate 1997, Comin-Chiaromonti & Gomes 2005). Syenites and nepheline syenites of miaskitic affinity (i.e., nepheline syenites containing zircon or titanite or molar $(\text{Na}_2\text{O} + \text{K}_2\text{O})/\text{Al}_2\text{O}_3 < 1$ in bulk-rock composition; Sørensen 1997, Le Maitre 2002) prevail in many occurrences in the Serra do Mar Alkaline Province (Almeida 1983, Brotzu et al. 2005). Mafic-ultramafic intrusive lithologies only occur as small, cumulate bodies associated with the syenitic stocks, such as in São Sebastião (Enrich et al. 2005) and Morro de São João (Brotzu et al. 2007), except for the Ponte Nova mafic-ultramafic massif, where felsic rocks are nearly absent (Azzone et al. 2009). The presence of agpaitic rocks (i.e., nepheline syenites and phonolites with molar $(\text{Na}_2\text{O} + \text{K}_2\text{O})/\text{Al}_2\text{O}_3 > 1$ and complex silicates of Zr, Ti, REE, and F and others volatiles; Sørensen 1997, Le Maitre 2002) is restricted to a few localities in this province, usually in small volumes associated with large miaskitic bodies, as in the Poços de Caldas, Itatiaia, and Passa Quatro massifs (Fig. 1A; Brotzu et al. 1992, Brotzu et al. 1997, Ulbrich & Ulbrich 2000, Enrich et al. 2005, Ulbrich et al. 2005).

The Monte de Trigo alkaline suite (86.6 Ma, Enrich et al. 2009) is a small, SiO_2 -undersaturated syenite-gabbro intrusive suite (Fig. 1A) that belongs to the Serra do Mar alkaline province. According to Enrich et al. (2009), the alkaline suite is composed of different pulses of undersaturated alkaline magmas. The oldest unit comprises a

cumulate nepheline-bearing olivine melagabbros, melatheralites (i.e., melanocratic nepheline gabbro, Le Maitre 2002) and clinopyroxenites with wide modal variations and layering structures. A leucocratic medium-to-coarse-grained nepheline syenite and nepheline-bearing alkali feldspar syenite intrude the cumulate mafic-ultramafic unit and compose most of the area of the suite. Alkali feldspar, hedenbergite, hastingsite, and biotite are early magmatic phases, whereas nepheline and analcime are late-crystallized phases. Accessory minerals include apatite, magnetite, and titanite and characterize a miaskitic association. Miaskitic and agpaitic nepheline microsyenite dykes cut the cumulate mafic-ultramafic body and the nepheline syenite

stock and are interpreted as late-stage differentiates of the nepheline syenite (Enrich et al. 2009).

NEPHELINE MICROSYENITE DYKES

Miaskitic nepheline microsyenites have hypidiomorphic to allotriomorphic texture with early crystallized alkali feldspar, hastingsite, titanite, apatite, and magnetite, followed by aegirine-augite and late-crystallized nepheline and sodalite. Agpaitic nepheline microsyenites are less abundant, vary from fine-to-medium-grained inequigranular seriate texture to equigranular aplitic texture, and the origin

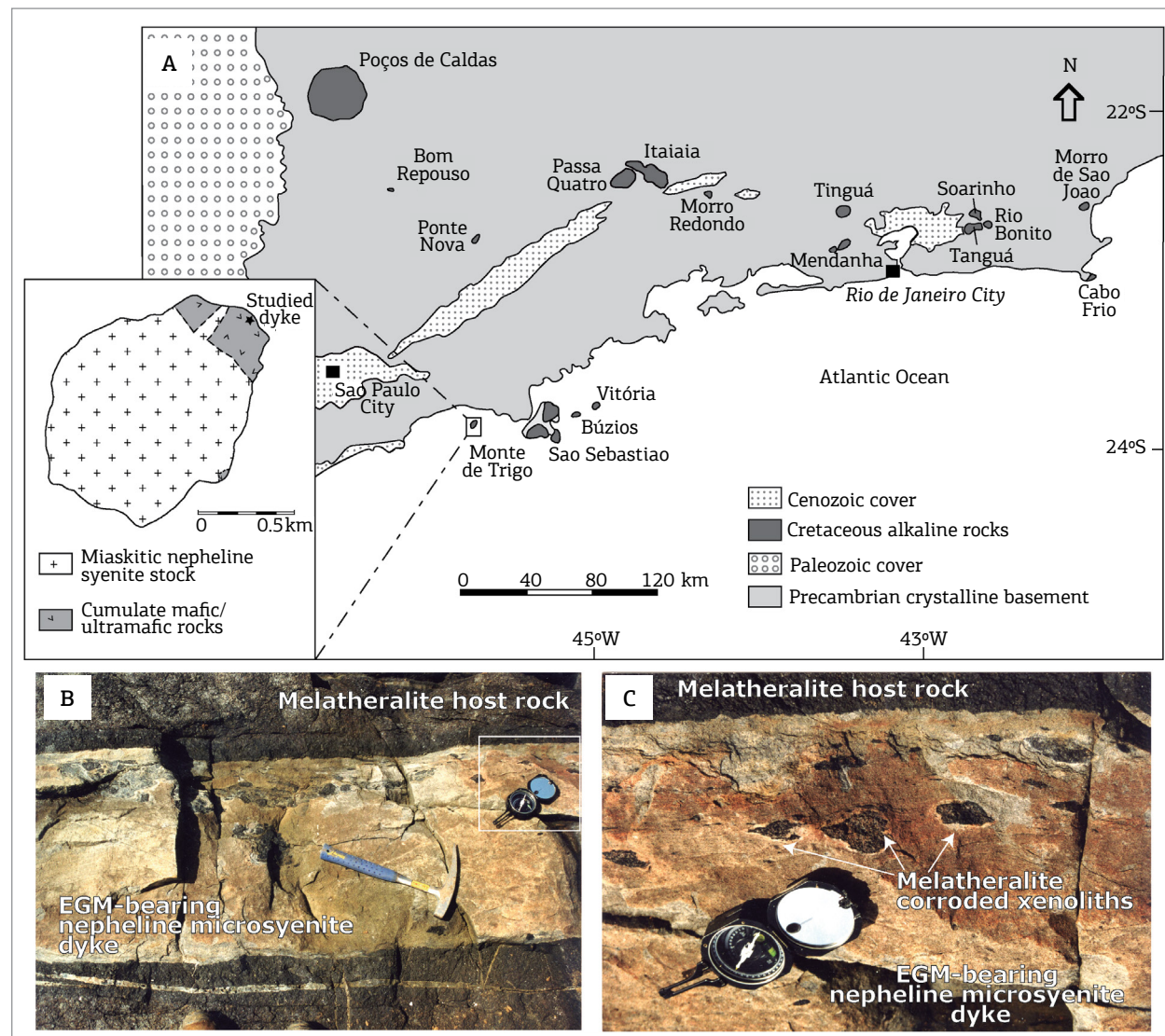


Figure 1. (A) Geological map of the Serra do Mar alkaline province and surrounding area in southeastern Brazil, modified from Almeida (1983). Inset: simplified geological map of Monte de Trigo Island (after Enrich et al. 2009); (B) Field relations of the EGM-bearing nepheline microsyenite dyke of the Monte de Trigo suite; (C) Detail of (B) showing corroded melatheralite xenoliths at the dyke border.

of these dykes is interpreted as having crystallized from a more evolved magma fraction than the miaskitic microsyenites ones. Alkali feldspar, nepheline, aegirine-augite, kato-phorite, magnetite, wöhlerite, hiortdahlite, and apatite are early crystallized phases, whereas sodalite, analcime, lävenite, zircon, zirconolite, baddeleyite, pyrochlore, and britholite are late-crystallized phases. Post-magmatic minerals include fluorite, rutile, calcite, and pyrite.

Only one agpaitic nepheline microsyenite dyke contains EGMs (Fig. 1B). This dyke is 50 cm wide and intrudes melatheralites at the northern coast of the island. The dyke exhibits an equigranular aplitic texture, which suggests co-precipitation of most of the phases. Major phases include mesoperthitic alkali feldspar (~45 vol%), nepheline (~35 vol%), and aegirine to aegirine-augite (~10 vol%). EGMs (~2 vol%) are the most abundant accessory phases. These minerals are colorless, subhedral, hexagonal- to round-shaped, and exhibit low birefringence and moderate relief (Fig. 2). Other accessory phases include Mn-rich magnetite and subhedral wöhlerite, each less than 1 vol%. Interstitial titanite, zircon, and britholite occur as late- to post-magmatic phases. The EGM-bearing nepheline microsyenite is classified as low agpaitic or transitional agpaitic (Khomyakov 1995, Sørensen 1997) in accordance with its accessory minerals.

Near the border, the EGM-bearing dyke shows an increase in the mafic mineral content, locally up to 25 vol%, as well as some mafic aggregates (Figs. 1C and 3A). The latter is composed of aegirine-augite and magnetite (Fig. 3B) and is interpreted as corroded and re-equilibrated xenoliths and/or xenocrysts of the melatheralite host-rock. Accessory minerals at the dyke border are EGMs and lävenite (Figs. 2C and 3B). Late-magmatic phases include poikilitic titanite, zirconolite, pyrochlore, and apatite.

The melatheralite host rock was transformed into a metasomatic granofels on a centimeter scale near the contact with the dyke, by its reaction with the alkaline volatile-rich liquid. Olivine, augite, and plagioclase from melatheralite were replaced by aegirine-augite, magnesiokatophorite, biotite, magnetite, and potassic feldspar (Fig. 3A). Aegirine-augite is the most abundant mineral within the first millimeter of the granofels. The granofels also has relict cores of augite with andradite rims, biotite, and magnesiokatophorite pseudomorphs after augite and masses of potassic feldspar after plagioclase (Fig. 3A and 3C).

ANALYTICAL METHODS

Major element analyses of the EGMs were performed on standard carbon-coated thin sections in a Jeol JXA-8600 electron microprobe using a Noran Voyager 4.1 automation

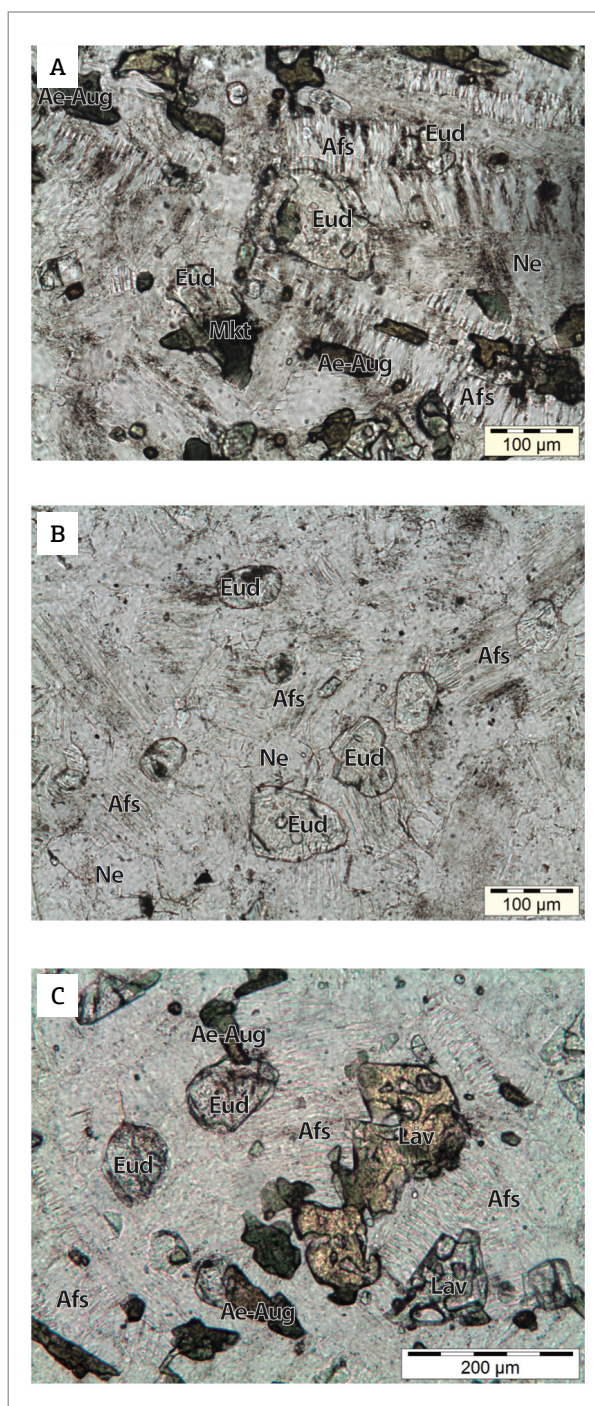


Figure 2. Photomicrographs of the EGMs from the Monte de Trigo alkaline suite. (A) Granular EGM in association with tabular mesoperthitic feldspar, prismatic aegirine-augite and subhedral magnesiokatophorite and nepheline grains (dyke border); (B) Rounded EGM grains with alkali feldspar and nepheline (dyke center); (C) Granular EGMs, anhedral lävenite, and prismatic aegirine-augite with alkali feldspar and nepheline (dyke border). Mineral abbreviations: Ae-aug, aegirine-augite; Afs, alkali feldspar; Eud, eudialyte; Låv, lävenite; Mkt, magnesiokatophorite; Ne, nepheline.

system at the Geoanalítica USP Core Facility of the University of São Paulo (USP). The analyses of standards and unknown samples were performed according to the electron microprobe settings of Williams (1996) (accelerating voltage of 25 kV and beam current of 100 nA) to properly quantify REE, HFSE, and other trace elements. The peak counting times were 10–20 s (F, Cl, Na, Si, K, Ca, Mn, Fe, Mg, Ti, and Al) and 40–60 s (La, Ce, Pr, Nd, Gd, Er, Yb, Y, Zr, Hf, Nb, Ta, U, Th, and Pb); the background counting times were half of the corresponding peak values. The Na and F contents were measured in the first minute of the analysis to prevent volatilization/migration due to the high probe current. A 30- μ m beam diameter was also employed to avoid volatilization/migration. The small EGM grain size in the studied samples together with the large beam diameter precluded a core-to-rim characterization. A combination of well-characterized natural and synthetic standards was used. The data were processed

using the PROZA procedure (Bastin et al. 1984). Special care was taken in the selection of the peak and background position to eliminate peak overlap. The detection limits were in the range of 0.01–0.03 wt%, except for F (up to 0.15 wt%).

After the removal of carbon coating from the thin sections, *in situ* trace-element analyses were performed on the same grain and as close as possible to the microprobe spot analysis using the laser ablation inductively coupled plasma mass spectrometry (LA-ICP-MS) at the Geoanalítica-USP Facility of the USP. The analytical work utilized a Perkin Elmer Elan 6100 DRC ICP-MS instrument coupled with a neodymium-doped yttrium aluminum garnet (Nd:YAG) laser (New Wave UP 213 AF) operating at a wavelength of 213 nm in a He+Ar atmosphere. Laser ablation was performed at 1.5 J/cm² at a pulse rate of 10 Hz. Due to the small grain size, and to avoid mineral inclusions, a predetermined line raster of 120 μ m with a 15- μ m beam diameter

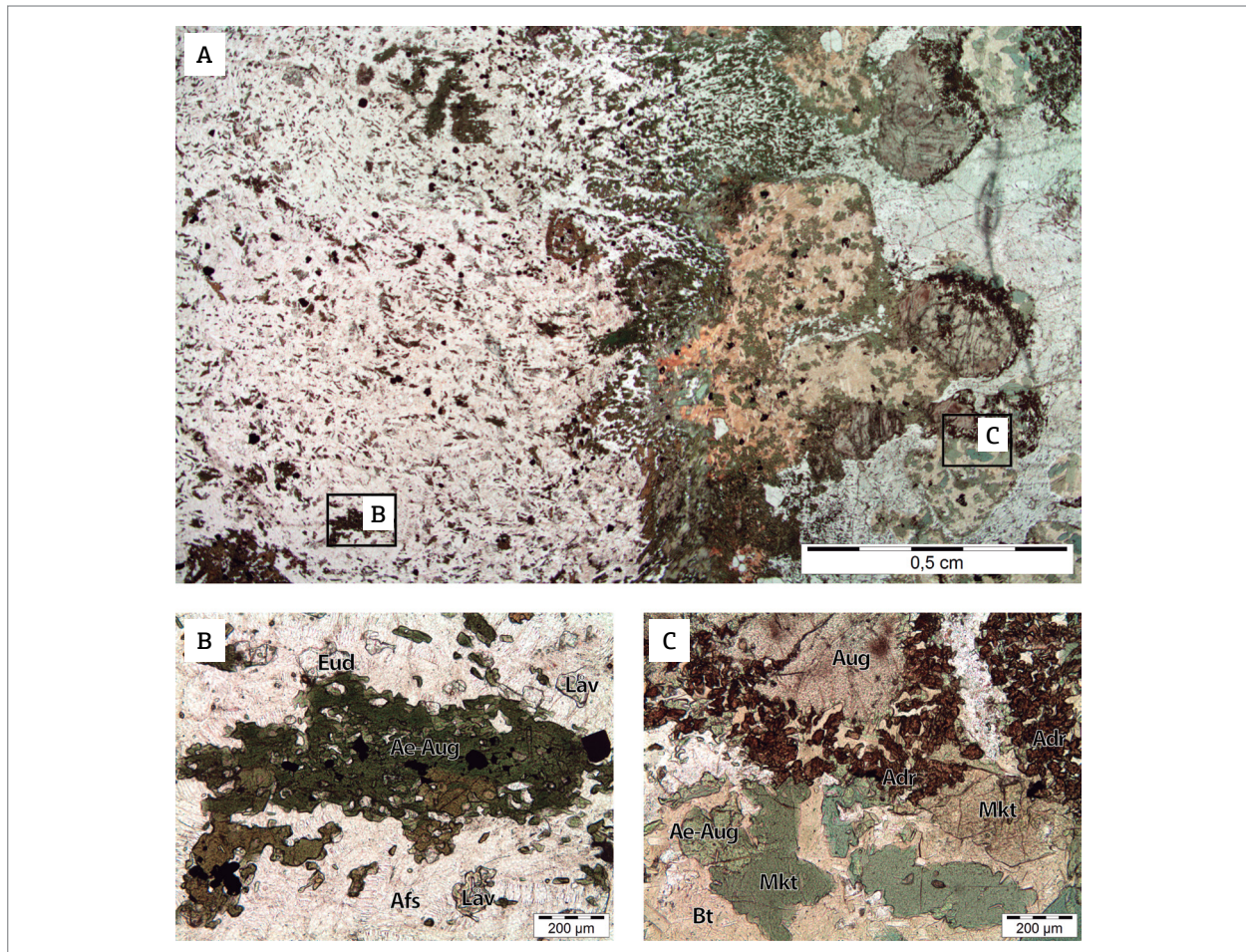


Figure 3 – (A) Contact between the EGM-bearing nepheline microsyenite dyke (left) and the melatheralite host rock (right) from Monte de Trigo; **(B)** Detail of (A) showing aegirine-augite and magnetite mafic aggregate near EGM and lávenite grains; **(C)** Detail of (A) showing the augite relict core with andradite border (top) and part of biotite, magnesiokatophorite, and aegirine-augite pseudomorph after augite (bottom). Mineral abbreviations: Ae-aug, aegirine-augite; Adr, andradite; Afs, alkali feldspar; Aug, augite; Bt, biotite; Eud, eudialyte; Låv, lávenite; Mkt, magnesiokatophorite.

at a 2- $\mu\text{m}/\text{s}$ scan speed was used. The Glitter 4.4.2 software (Van Achterbergh et al. 2001) was used for data processing with National Institute of Standards and Technology (NIST) SRM 610 as the external standard and ^{42}Ca as the internal standard using values for CaO from the electron microprobe analysis for the minerals. A linear adjustment was selected as the interpolation method for drift control and quantification. The relative errors (1σ) were in the range of 5–10% for most of the trace elements. Detection limits are usually between 0.1 and 2 ppm, except for Mg and Zn, with values up to 20 ppm. Whenever an element was analyzed with microprobe and LA-ICP-MS (e.g., Hf, Ta, Pb, Mg, and some REE), the more precise data from LA-ICP-MS were preferred.

EGM structural formulae were calculated according to Johnsen & Grice (1999) and Johnsen et al. (2001) based on 29 cations (sum of Si, Al, Zr, Ti, Hf, Nb, W and Ta) and constraining all Fe and Mn to be divalent.

The bulk-rock compositions of major and some trace elements were analyzed in a fused glass disc and pressed powder pellets using a Philips PW 2400 X-ray fluorescence spectrometer at the Geoanalítica-USP Facility of the USP using standard methods as described by Mori et al. (1999). Weight loss on ignition (LOI) was evaluated using standard gravimetric techniques. Trace elements and REE were analyzed in a Perkin Elmer Elan 6100 DRC ICP-MS at the Geoanalítica-USP Facility of the USP following the procedures delineated in Navarro et al. (2008).

RESULTS

Bulk-rock composition

Bulk-rock data for selected agpaitic dykes from Monte de Trigo are presented in Table 1. These rocks have SiO_2 contents varying from 57.6 wt% to 59.9 wt% and $\text{Na}_2\text{O} + \text{K}_2\text{O}$ from 13.2 wt% to 14.4 wt%. All dykes are peralkaline (molar $(\text{Na}_2\text{O} + \text{K}_2\text{O})/\text{Al}_2\text{O}_3 > 1$) and contain EGMs, wöhlerite, lävenite, and/or hiortdahlite. Major compositional differences among the dykes are controlled by the amounts of mafic and accessory phases they contain. The least evolved agpaitic variety is EGM-free, aegirine-rich (~7 vol%), has low mg# (molar $\text{MgO}/(\text{MgO} + \text{FeOt}) = 0.09$), REE (267 ppm) and Zr (969 ppm) contents, and relatively high SiO_2 (59.91 wt%) and Fe_2O_3 (5.38 wt%) contents. The EGM-free evolved variety has high REE contents (569 ppm), which are associated with their relatively high britholite modal content.

The EGM-bearing nepheline microsyenite dyke (peralkaline index = 1.08) has a sodic character ($\text{Na}_2\text{O}/\text{K}_2\text{O} = 2.5$), with the lowest K_2O content and highest Na_2O content

Table 1. Major (wt.%) and trace element (ppm) bulk compositions of the studied EGM-bearing nepheline microsyenite dyke (center), the melatheralite host-rock and representative EGM-free nepheline microsyenite from Monte de Trigo alkaline suite

Sample	mtr01b ^a	mtr04c ^b	mtr01h ^b	mtr01d ^c
SiO_2	57.61	59.91	57.58	40.45
TiO_2	0.12	0.28	0.23	2.91
Al_2O_3	21.09	17.76	21.12	10.9
Fe_2O_3	4.15	5.38	3.47	14.62
MnO	0.233	0.214	0.213	0.189
MgO	0.04	0.27	0.12	12.79
CaO	0.69	0.94	0.77	15.17
Na_2O	10.98	7.8	10.13	0.91
K_2O	4.4	5.4	4.86	0.47
P_2O_5	<0.003	0.029	0.004	0.19
LOI	0.43	0.64	0.60	0.60
Total	99.75	98.63	99.10	99.20
P.I. ^d	1.08	1.05	1.04	0.18
V	5	5	4	480
Cr	<2	<2	<2	561
Co	<3	<3	<3	67
Ni	2	<2	2	231
Sc	<4	4	<4	34
Zn	130	117	180	78
Sr	18	20	44	669
Ga	59	43	55	18
Rb	297	243	282	11.4
Y	51.3	36.4	73.7	17.9
Zr	2,672	969	2,611	138
Nb	383	182	314	13
Cs	1.62	1	4.29	0.2
Ba	23	21.7	49.6	169
La	86.9	42.6	157	16.5
Ce	210	130	276	39.8
Pr	12.1	12.8	21.8	6.14
Nd	35	46.7	63	28.4
Sm	6.42	8.46	10.4	6.54
Eu	0.4	0.45	1.55	2.04
Gd	6.18	7.32	8.83	6.13
Tb	1.25	1.2	1.69	0.83
Dy	7.8	6.92	10.3	4.31
Ho	1.8	1.45	2.3	0.77
Er	5.59	4.21	7.12	1.86
Tm	0.91	0.62	1.12	0.23
Yb	5.96	4.03	7.27	1.3
Lu	0.93	0.64	1.06	0.19
Hf	57.9	23.7	52.9	4.2
Ta	26.5	12.7	18	1.51
Pb	25.3	05.4	43	01.6
Th	3.54	3.64	43.4	0.95
U	2.75	2.81	18.9	0.85

^aEGM-bearing nepheline microsyenite dyke (centre); ^bEGM-free nepheline microsyenite dyke; ^cMelatheralite (wall rock of the EGM-bearing nepheline microsyenite dyke); ^dPeralkaline index: molar $(\text{Na}_2\text{O} + \text{K}_2\text{O})/\text{Al}_2\text{O}_3$.

among the dykes (4.4 wt% and 10.98 wt%, respectively). This dyke has an extremely low mg# (0.02), Ba (23 ppm), and Sr (18 ppm) contents and high Zr (2672 ppm), Nb (383 ppm), Rb (297 ppm), Y (51.3 ppm), and REE (381.2 ppm) contents (Table 1). The chondrite-normalized REE pattern exhibits light REE enrichment, with a La_N/Yb_N ratio of 9.9 and with a negative Eu/Eu* (C1 chondrite-normalized ratio of Eu/(Sm*Gd)^{1/2}) anomaly of 0.20.

The melatheralite host rock has cumulate diopside and olivine crystals and exhibits high MgO (12.79 wt%), Fe₂O₃ (14.62 wt%), and CaO (15.17 wt%) contents, and low Na₂O (0.91 wt%) and K₂O (0.47 wt%) contents. Trace elements include high Cr (561 ppm), Ni (231 ppm), and Sr (669 ppm) contents. The REE content is low (Σ REE = 115 ppm) and has a low light REE enrichment, with a La_N/Yb_N ratio of 8.6 and no europium anomaly (Eu/Eu* = 0.98).

EGM compositions

The major and trace element compositions of the EGMs from Monte de Trigo are listed in Table 2. The studied EGMs have

high SiO₂ (46.02–48.07 wt%) content with significant amounts of ZrO₂ (11.11–12.11 wt%), Na₂O (10.73–11.86 wt%), and CaO (10.76–12.51 wt%). In addition, they contain nearly equal concentrations of FeO (3.13–4.83 wt%) and MnO (3.01–4.52 wt%). Other major elements include Nb₂O₅ (1.28–3.09 wt%), REE₂O₃ (2.00–3.43 wt%), and Cl (1.67–1.85 wt%).

The most significant minor and trace element data include TiO₂ (0.16–0.34 wt%), HfO₂ (0.12–0.26 wt%), Ta₂O₅ (0.05–0.29 wt%), Y₂O₃ (0.37–0.86 wt%), PbO (0.09–0.22 wt%), K₂O (0.23–0.50 wt%), F (0.13–0.31 wt%), Mg (60–3582 ppm), Sr (108–2,699 ppm), Zn (401–852 ppm), and W (216–882 ppm).

Compositions of other accessory phases

Wöhlerite [Na₈(Mn,Ca,Fe,Ti)₄(Zr,Nb)₄(Si₂O₇)₄(O,F)₈] and lävenite [Na₄(Ca,Mn,Fe)₈Zr₂(Nb,Ti)₂(Si₂O₇)₄O₄F₂(F,O)₂], minerals of the cuspidine group (Mellini & Merlino 1979, Mellini 1981, Merlino & Perchiazzi 1988, Chakhmouradian et al. 2008), are the major accessory phases that crystallize contemporaneously with EGMs in the studied dyke.

Table 2. Compositions of the EGMs from the Monte de Trigo alkaline suite. Representative analysis of lävenite (Låv) and wöhlerite (Wöh) were also included

Analysis ^a	1	2	3	4	5	6	7	8	9
wt% ^b									
SiO ₂	47.62	46.60	47.12	47.26	46.02	46.86	46.75	46.83	47.48
Al ₂ O ₃	<0.01	<0.01	<0.01	<0.01	<0.01	<0.01	0.02	<0.01	<0.01
TiO ₂	0.33	0.22	0.25	0.34	0.16	0.23	0.23	0.21	0.23
ZrO ₂	11.94	11.78	11.85	11.98	11.57	11.78	11.77	11.84	11.78
HfO ₂	0.23	0.22	0.25	0.22	0.25	0.21	0.23	0.26	0.24
Nb ₂ O ₅	2.05	2.52	2.46	1.91	3.09	2.57	2.71	2.68	2.35
Ta ₂ O ₅	0.20	0.23	0.19	0.17	0.22	0.20	0.16	0.25	0.25
Y ₂ O ₃	0.86	0.79	0.86	0.86	0.73	0.80	0.82	0.80	0.85
REE ₂ O ₃	2.93	3.36	3.13	2.38	3.43	3.09	3.00	2.86	2.72
FeO	3.33	3.17	3.24	3.44	3.28	3.56	3.51	3.13	3.28
MnO	4.00	4.34	4.23	3.88	4.52	4.05	4.20	4.30	4.09
CaO	12.51	12.01	11.96	12.04	12.01	12.04	11.84	12.27	12.12
Na ₂ O	10.73	11.37	11.50	11.86	11.33	11.45	11.48	11.29	11.46
K ₂ O	0.24	0.23	0.25	0.28	0.27	0.33	0.23	0.23	0.24
Cl	1.75	1.73	1.73	1.78	1.67	1.68	1.74	1.75	1.77
F	0.20	0.25	0.23	0.27	0.17	0.14	0.18	0.24	0.31
H ₂ O ^c	1.75	1.66	1.71	1.65	1.75	1.81	1.74	1.68	1.63
-O=F,Cl	0.48	0.50	0.49	0.51	0.45	0.44	0.47	0.50	0.53
Total ^d	100.43	100.27	100.75	99.97	100.35	100.67	100.39	100.39	100.51
Structural formulae (a.p.f.u.) ^e									
Si	25.226	25.126	25.150	25.227	25.024	25.133	25.106	25.096	25.218
Zr	3.085	3.097	3.084	3.119	3.066	3.080	3.081	3.094	3.051
Ti	0.129	0.087	0.101	0.135	0.064	0.092	0.094	0.083	0.093
Nb	0.490	0.615	0.593	0.460	0.759	0.622	0.657	0.650	0.565
Fe	1.476	1.429	1.446	1.534	1.491	1.596	1.577	1.402	1.455
Mn	1.794	1.981	1.913	1.756	2.083	1.838	1.912	1.951	1.839

Continue...

Table 2. Continuation

Analysis^a	1	2	3	4	5	6	7	8	9
REE	0.559	0.652	0.600	0.471	0.673	0.597	0.580	0.569	0.536
Ca	7.098	6.937	6.839	6.886	6.996	6.916	6.811	7.046	6.896
Y	0.242	0.226	0.244	0.243	0.211	0.228	0.234	0.228	0.241
Na	11.016	11.890	11.899	12.277	11.939	11.910	11.951	11.724	11.802
K	0.163	0.159	0.172	0.189	0.184	0.228	0.155	0.156	0.163
F	0.340	0.428	0.390	0.447	0.296	0.232	0.299	0.402	0.521
Cl	1.571	1.583	1.568	1.613	1.539	1.531	1.587	1.591	1.594
H	3.089	2.989	3.042	2.940	3.165	3.237	3.114	3.007	2.885
Trace elements (ppm)^f									
Mg	103	248	146	72	154	181	150	157	
Sc	25	27	25		29	29	26		
Zn	467	535	477		495	505	401		
Ga	73	97	91		106	96	87		
Rb	28	31	31		18	27	21		
Sr	117	152	112		121	108	127		
Mo	32	43	48		116	62	43		
Cs	17	16	18		10	15	17		
Ba	4	8	6		5	6	4		
La	7,689	9,253	8,198	5,986	9,427	8,217	7,969	7,973	7,282
Ce	10,019	11,283	10,621	9,050	11,880	10,559	10,032	10,732	10,083
Pr	802	928	849	581	927	846	783	667	786
Nd	2,362	2,734	2,577	2,092	2,716	2,495	2,402	2,298	2,306
Sm	527	574	541		543	557	532		
Eu	32	41	39		38	36	39		
Gd	632	714	642	902	651	669	662	1,006	842
Tb	140	158	151		144	147	146		
Dy	1,009	1,088	1,079		1,029	1,032	1,094		
Ho	232	247	262		247	236	254		
Er	692	728	768	883	750	731	769	840	936
Tm	109	119	122		115	114	123		
Yb	764	776	837	843	815	765	822	957	1,019
Lu	100	098	112		107	102	108		
W	377	402	409		882	634	216		
Pb	1,117	1,425	1,267	882	1,345	1,229	1,321	1,550	1,402
Th	7	6	9		7	8	7		
U	25	28	31		25	29	33		
Analysis	10	11	12	13	14	15		Låv	Wöh
wt%									
SiO ₂	47.64	46.84	48.07	48.28	47.46	46.27		29.39	28.91
Al ₂ O ₃	0.07	<0.01	0.21	0.02	0.07	0.02		<0.01	<0.01
TiO ₂	0.24	0.18	0.24	0.22	0.30	0.17		3.61	1.37
ZrO ₂	11.40	11.81	11.11	12.11	12.02	12.01		27.08	15.23
HfO ₂	0.23	0.23	0.12	0.14	0.14	0.13		0.27	0.34
Nb ₂ O ₅	2.41	2.57	1.77	1.55	1.28	2.56		3.38	13.55
Ta ₂ O ₅	0.22	0.29	0.05	0.07	0.08	0.06		0.09	0.47
Y ₂ O ₃	0.79	0.84	0.47	0.39	0.37	0.39		0.36	0.32
REE ₂ O ₃	2.75	2.90	2.47	2.00	1.99	2.86		0.145	0.811
FeO	3.20	3.19	4.08	4.83	4.76	4.27		3.77	0.42
MnO	4.09	4.25	3.21	3.04	3.01	3.65		4.03	1.59
CaO	11.82	12.15	10.76	11.42	11.77	11.86		13.02	25.79
Na ₂ O	11.52	11.52	11.68	11.24	11.48	10.92		12.04	8.05

Continue...

Table 2. Continuation

Analysis	10	11	12	13	14	15		Låv	Wöh
K ₂ O	0.45	0.25	0.43	0.37	0.50	0.24		<0.01	<0.01
Cl	1.70	1.76	1.75	1.85	1.81	1.80		<0.01	<0.01
F	0.14	0.13	0.15	0.29	0.20	0.18		4.54	3.72
H ₂ O ^c	1.82	1.78	1.79	1.64	1.69	1.68			
-O=F,Cl	0.44	0.45	0.46	0.54	0.49	0.48		1.91	1.57
Total ^d	100.39	100.45	98.87	99.92	99.30	99.58		99.81	99.02
Structural formulae (a.p.f.u.)^e									
Si	25.306	25.135	25.568	25.401	25.399	25.090			
Zr	2.953	3.090	2.881	3.107	3.136	3.175			
Ti	0.095	0.073	0.097	0.086	0.120	0.069			
Nb	0.579	0.624	0.425	0.369	0.311	0.627			
Fe	1.421	1.432	1.814	2.124	2.129	1.937			
Mn	1.841	1.930	1.445	1.356	1.366	1.676			
REE	0.544	0.574	0.477	0.381	0.394	0.562			
Ca	6.728	6.984	6.129	6.434	6.746	6.891			
Y	0.222	0.238	0.134	0.108	0.106	0.112			
Na	11.858	11.979	12.041	11.463	11.914	11.475			
K	0.307	0.169	0.292	0.250	0.339	0.168			
F	0.240	0.217	0.252	0.476	0.337	0.309			
Cl	1.531	1.599	1.581	1.647	1.640	1.657			
H	3.228	3.184	3.167	2.877	3.023	3.034			
Trace elements (ppm)									
Mg	127	60	1,547	1,179	3,582	1,301		3,819	083
Sc			29	27		25		63	35
Zn			831	732		852		329	27
Ga			76	61		86		<01	23
Rb			121	73		56		<01	<01
Sr			2,161	2,315		2,699		75	12
Mo			41	41		106		18	24
Cs			39	31		27			
Ba			3	1		4		<1	<1
La	7,418	7,930	7,967	5,868	5,679	8,993		54	1,018
Ce	10,519	10,912	8,639	7,120	7,539	10,257		120	2,515
Pr	743	803	675	586	675	817		14	304
Nd	2,435	2,452	1,870	1,750	1,938	2,325		56	1,179
Sm			362	343		413		24	304
Eu			27	24		28		3	20
Gd	685	937	402	355	564	427		65	288
Tb			74	64		73		26	64
Dy			465	403		445		251	449
Ho			94	78		94		66	98
Er	944	1,032	234	215	350	238		216	299
Tm			33	34		36		38	47
Yb	755	711	237	226	307	241		294	337
Lu			26	28		27		36	45
W			232	353		576		7	127
Pb	1,439	1,374	1,537	1,644	1,476	2,011		19	52
Th			58	112		130		33	9
U			12	8		7		21	69

^aThe EGM analyses 1–11 and the wöhlertite are from the dyke center (sample mtr01b); the EGM analyses 12–15 and the låvenite are from the dyke border (sample mtr01a); ^bmajor element contents (wt.%) were determined by electron probe micro-analyzer (EPMA); ^cestimated considering Cl+F+OH=5 a.p.f.u.; ^dincludes H₂O and trace elements; ^estructural formulae calculated on the basis of 29 cations (Si+Al+Zr+Ti+Hf+Nb+W+Ta), with all Fe and Mn constrained to be divalent; ^ftrace element (ppm) as well as HfO₂, Ta₂O₅ and PbO (wt%) were determined by inductively coupled plasma mass spectrometry (ICP-MS), except from analyses 4, 8, 9, 10, 11, and 14, that were only EPMA data are available.

Representative analyses of wöhlerite and låvenite are presented in Table 2. These phases have lower SiO_2 and higher ZrO_2 contents than EGMs. Wöhlerite has higher Nb_2O_5 and CaO contents than låvenite does, whereas the latter has high MnO , FeO , and Na_2O contents. Both minerals have almost no LILE, but they are enriched to a variable degree in REE. Wöhlerite contains greater amounts of light REE than låvenite does. The $\text{La}_{\text{N}}/\text{Yb}_{\text{N}}$ ratios of wöhlerite and låvenite are 2.05 and 0.12, respectively, which are significantly lower than the values for EGMs from the dyke center (4.8–8.0), EGMs from the dyke border (12.5–25.0) and the bulk-rock composition (9.9). The Eu/Eu^* anomaly is somewhat similar to that observed in the EGMs and bulk-rock analysis. Låvenite also has high contents of Mg (3,819 ppm) and Zn (329 ppm).

DISCUSSION

EGM compositional variation and molecular components

According to the calculated structural formulae (Table 2), Si contents are sufficient to fill 25 tetrahedral positions, whereas the Zr (plus minor content of Hf) and Ca amounts fill the Z and $M(1)$ positions, respectively. In the X site, Cl prevails over F.

The most extensive variation in the EGM composition from Monte de Trigo involves Fe and Mn at the $M(2)$ site and Si and Nb at the $M(3,4)$ site (Fig. 4). Both variations correspond to the solid solution between eudialyte and kentbrooksite components, recognized as the major substitution of the EGMs worldwide by Johnsen et al. (1998) and Johnsen & Grice (1999), although excluding the F and Cl contents. In fact, some analyses present Mn as dominant cation in $M(2)$ site with the X site occupied by Cl, which probably is a mineral still not approved by the International Mineralogical Association. A slight excess of Zr from the Z site could be located with Nb and Si in the $M(3,4)$ site, together with minor to trace contents of Ti, Ta, and W.

Other significant major element variations in the EGMs from Monte de Trigo occur at the $N(1-5)$ site. Most of the 15 positions of the $N(1-5)$ sites are filled with Na, which varies from 11.02 to 12.28 apfu . The remaining positions may include other elements, such as REE, Y, Ca, and Mn, probably at the $N(4)$ site (Rastsvetaeva 2007). The sum of the Fe and Mn contents (3.259 to 3.613 apfu) exceeds the three available $M(2)$ positions. This excess suggests that small amounts of the georgbarsanovite component are present in the solid solution, in which Mn is located at the $N(4)$ site (Khomyakov et al. 2005, Rastsvetaeva 2007). Similarly, the Ca content (6.129 to 7.098 apfu) exceeds the required amount to fulfill the six positions of the $M(1)$ site (Fig. 4),

with the surplus Ca most likely located at the $N(4)$ site, composing the feklichevite member (Pekov et al. 2001).

The $N(4)$ site also includes REE (0.381 to 0.673 apfu) and Y (0.106 to 0.244 apfu), which indicates the presence of a zirsilite-(Ce) component (Khomyakov et al. 2003). Light REE enrichment is observed in the C1 chondrite-normalized REE diagram (Fig. 5A), with $\text{La}_{\text{N}}/\text{Sm}_{\text{N}}$ ratios ranging from 9.1 to 13.7 and $\text{Gd}_{\text{N}}/\text{Lu}_{\text{N}}$ ratios ranging from 0.71 to 1.95. A clearly marked negative Eu/Eu^* anomaly is present, with values varying from 0.17 to 0.23.

Thus, the EGMs from Monte de Trigo are best represented by a complex solid solution involving eudialyte, feklichevite, zirsilite-(Ce), georgbarsanovite, and kentbrooksite components (Fig. 4). Part of the Mn content of the EGMs may be responsible for the formation of minor quantities of the manganoeudialyte member (Nomura et al. 2010) rather than kentbrooksite to compensate for the Nb deficiency, assuming all of the Nb-bearing components are present. The EGMs from the dyke border are more enriched in the eudialyte component, whereas the EGMs from the dyke center are more enriched in the feklichevite, zirsilite-(Ce) and kentbrooksite components (Fig. 4).

The trace element contents normalized according to the bulk composition of the host dyke are shown in Figure 5B. The EGMs from the dyke border have significantly higher contents of Sr, Th, Zn, and Mg and significantly lower contents of Hf, Ta, and heavy REE than those from the dyke center. The low K, Rb, and Ba EGM/bulk-rock ratios suggest an incompatible behavior, i.e., they are not incorporated in the EGM structure. Thus, the andrianovite component, an EGM similar to kentbrooksite and zirsilite-(Ce), but with K located at the $N(4)$ site (Khomyakov et al. 2008), is irrelevant in the composition of the EGMs from Monte de Trigo, despite the high K and Rb contents of the bulk rock (Table 1). This finding suggests that K and Rb prefer other minerals, such as alkali feldspar. The contents of Mg, Zn, Ga, Sr, Th, and U in EGMs are slightly higher than the ones in the host rock, which suggests that they are neutral to compatible in the EGM structure, whereas Pb is highly compatible, with EGM/bulk-rock ratios near 100, probably because the ionic radius of Pb (Shannon 1976) is similar to the size of the $N(4)$ site (Johnsen & Grice 1999).

Petrologic implications

The EGMs from Monte de Trigo are distinguished by relatively high contents of Ca, moderate enrichment of Nb and REE, and a somewhat low content of Na when compared with the compositions from other localities worldwide (e.g., Deer et al. 1986, Johnsen & Gault 1997, Johnsen & Grice 1999, Wu et al. 2010, Schilling et al. 2011b). The EGMs from Monte de Trigo do have Na, Nb, Ca, and REE contents similar to

those of the EGMs from Langesundsfjord and North Qôroq (Fig. 4) (Bollingberg et al. 1983, Coulson & Chambers 1996, Coulson 1997, Wu et al. 2010).

The Na-poor and Ca-rich composition of the analyzed EGMs may be a consequence of transitional agpaitic magma composition. The accessory mineral assemblage

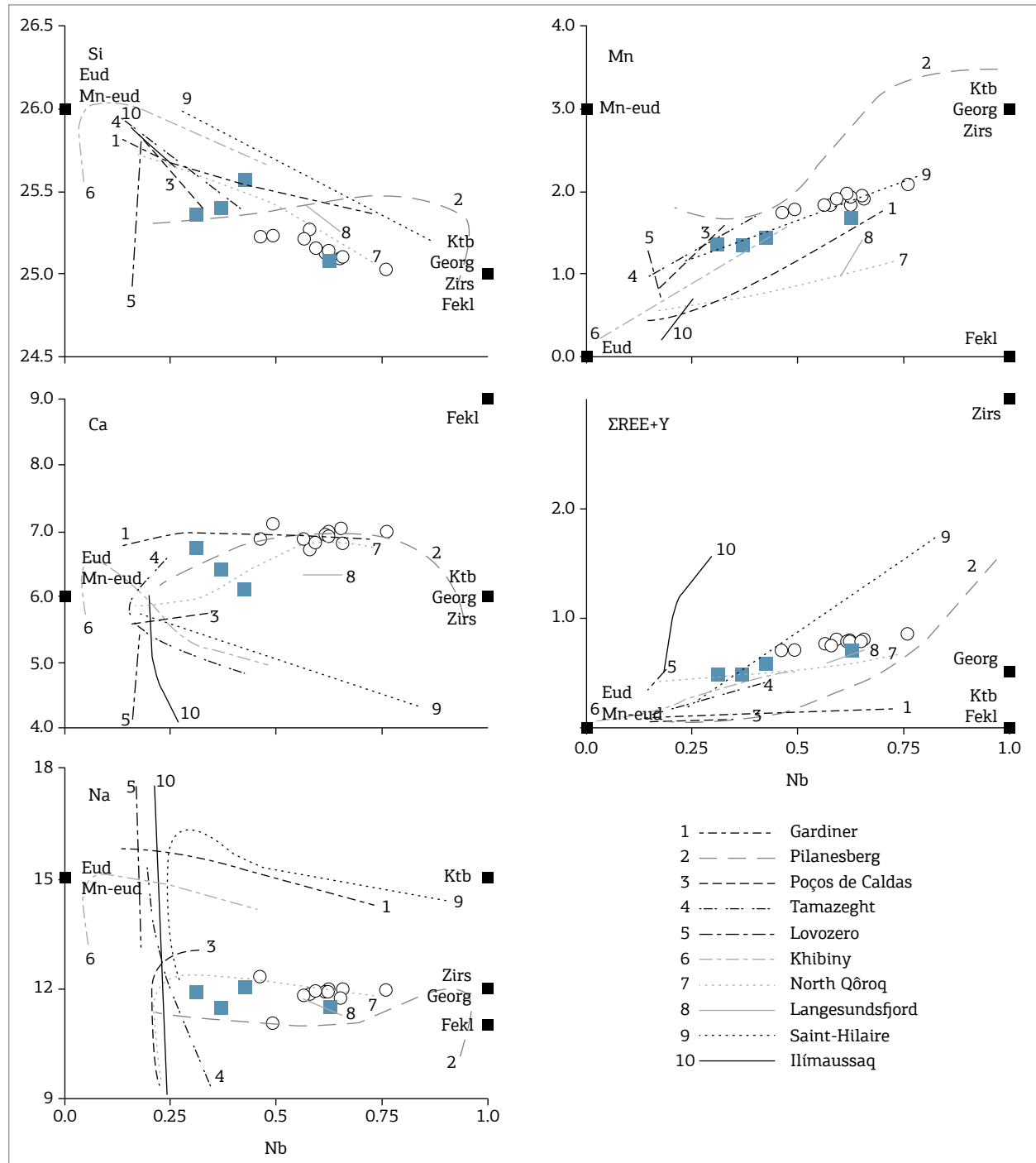


Figure 4. Plot of Nb vs. Si, Mn, Ca, Σ REEs+Y and Na (apfu) for the EGMs from Monte de Trigo. Blue squares, the EGMs from the dyke border; open circles, the EGMs from the dyke center; black squares, theoretical end-members of the EGMs. Trend lines of the worldwide EGM compositions are compiled from Coulson & Chambers (1996), Gualda & Vlach (1996), Coulson (1997), Johnsen & Gault (1997), Olivio & Williams-Jones (1999), Johnsen & Grice (1999), Mitchell & Lifervovich (2006), Marks et al. (2008), Schilling et al. (2009, 2011b), and Wu et al. (2010). Component abbreviations: eud, eudialyte; Mn-eud, manganoeudialyte; fekl, feklichevite; ktb, kentbrooksite; georg, georgbarsanovite; zirs, zirssilite-(Ce).

from Monte de Trigo, as well as those from Langesundsfjord and North Qôroq, includes complex Na-Ca-Zr-F silicate minerals, such as wöhlerite and lävenite (Coulson 1997, Enrich et al. 2009, Andersen et al. 2010), which is typical of transitional agpaitic rocks (Sørensen 1997, Andersen et al. 2010, Marks et al. 2011). This assemblage suggests that the miaskitic to agpaitic transition in the Monte de Trigo alkaline suite follows the increasing fluorine trend of Andersen et al. (2010). The EGM crystallization along this fluorine trend, according to these authors, can occur if chlorine or HCl activity is sufficiently high. This seems to be the case for the EGMs from Monte de Trigo, as evidenced by their relatively high Cl content.

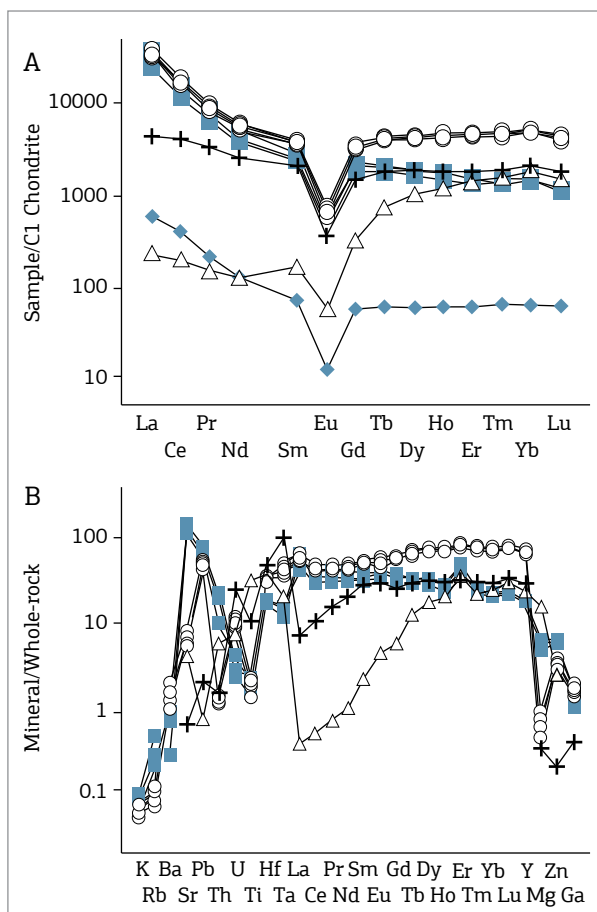


Figure 5. (A) C1 chondrite-normalized REE diagram for EGMs. Chondrite values are from McDonough & Sun (1995); (B) Bulk-rock-normalized multi-element diagram of the EGMs from Monte de Trigo. The bulk-rock values are from the EGM-bearing nepheline microsyenite dyke center sample (Table 1). Blue squares, the EGMs from the dyke border; open circles, the EGMs from the dyke center. The bulk-rock data from the dyke center (blue diamonds), lävenite (open triangle) and wöhlerite (black cross) are also plotted for comparison.

Most of the trace element contents of the EGMs from Monte de Trigo vary within the ranges of EGMs from other localities (Wu et al. 2010, Schilling et al. 2011b), especially the HFSEs and REE. Major differences of the analyzed EGMs include low-Sr and Ba contents and a negative Eu/Eu* ratio (Fig. 6). These differences are also found in the bulk composition of the EGM-bearing nepheline microsyenite dyke (Table 1), which suggests that EGMs crystallized in an environment where Eu, Sr, and Ba were already depleted. This depletion could be assigned to previous extensive fractionation of plagioclase and/or alkali feldspar (e.g., Blundy & Wood 1991, Bédard 2006, Brotzu et al. 2007, Henderson & Pierozynski 2012, Carvalho & Janasi 2012) from the parental melt, similar to the interpretation by Schilling et al. (2011b) regarding the same features observed in the EGMs from Ilímaussaq and Mont Saint-Hilaire.

Extensive plagioclase fractionation is usually related to alkaline massifs with a basanite/alkali basalt parental melt, whereas it is absent for nepheline parental magma (Marks et al. 2011, Schilling et al. 2011a, 2011b). Thus, EGMs that are crystallized from agpaitic residual liquids derived from basanite/alkali basalt and nepheline parental magmas should present Sr-poor and Sr-rich trends, respectively. The compositional trends for EGMs from several occurrences are shown in the FeO-SrO-REE₂O₃ diagram (Fig 7). The FeO-rich corner characterizes the composition of early magmatic EGMs, as indicated by Schilling et al. (2011b). Both REE- and Sr-rich end-members of EGMs are related to late-magmatic and/or post-magmatic hydrothermal fluids, as are, for example, the final compositions of the EGM trends from the Pilanesberg and Saint-Hilaire complexes (Olivio & Williams-Jones 1999, Mitchell & Liferovich 2006, Grice & Gault 2006, Schilling et al. 2011b). The Sr-poor EGM trends found at Saint-Hilaire and Ilímaussaq reflect their basanite/alkali basalt parental magma (Larsen & Sørensen 1987, Bailey et al. 2001, Schilling et al. 2011a). Conversely, the Sr-rich EGM trends found at Poços de Caldas, Gardiner, Khibina and Lovozero could be linked to their nepheline parental magma (Nielsen 1980, Kramm & Kogarko 1994, Sørensen 1997, Ulbrich et al. 2005, Kogarko et al. 2010). The EGMs from Monte de Trigo have relative Fe and REE enrichment that, together with the EGM texture, agrees with its magmatic origin. The Sr-poor EGM trends found in Monte de Trigo reflect their basanite/alkali basalt parental magma. A mafic dyke with basanite composition has already been described in Monte de Trigo (Thompson et al. 1998, Enrich et al. 2009), and it probably represents the parental magma for this alkaline suite. Again, the EGMs from Monte de Trigo are plotted close to the north Qôroq and Langesundsfjord EGM data.

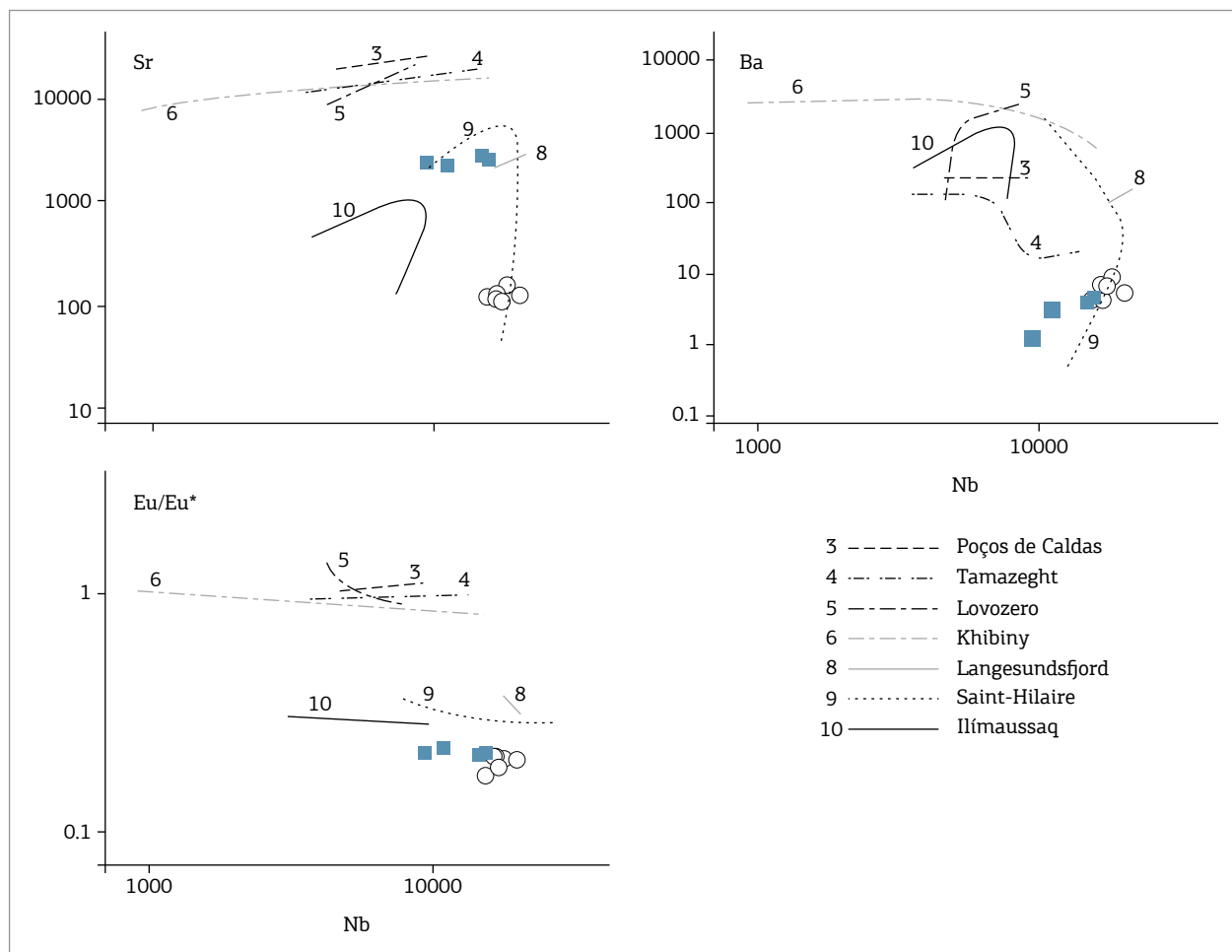


Figure 6. Plot of Nb vs. Si, Mn, Ca, Σ REE+Y and Na (ppfu) for the EGMs from Monte de Trigo. Trend lines of the worldwide EGM compositions are compiled from Gualda & Vlach (1996), Johnsen & Gault (1997), Johnsen & Grice (1999), Marks et al. (2008), Schilling et al. (2009, 2011b), and Wu et al. (2010). Blue squares, the EGMs from the dyke border; open circles, the EGMs from the dyke center.

Some additional considerations about the compositional differences between the EGMs from the dyke border in relation to those from the center also could be made. The EGMs from the dyke border have the highest Mg (up to 3,582 ppm) and Zn (up to 852 ppm) contents of the worldwide EGMs (up to 1,000 ppm and 200 ppm for Mg and Zn, respectively; Deer et al. 1986, Gualda & Vlach 1996, Johnsen et al. 1998, Johnsen & Grice 1999, Ridolfi et al. 2003, Bulakh & Petrov 2004, Marks et al. 2008, Wu et al. 2010, Schilling et al. 2011b). Such high Mg and Zn contents, associated to relatively high Fe and Sr in these EGMs, could be related to the incorporation and reaction of the melatheralite xenoliths, as these elements are more abundant in the melatheralite (Table 1). The local-scale reaction due to the diffusive exchange between the melatheralite and the agpaitic magma at dyke border are suggested by the presence of corroded xenoliths (Fig. 1C), large mafic aggregates (Fig. 3B) and metasomatic granofels (Fig. 3A), and by the increase in modal mafic mineral content, up

to 25% in volume. In addition, lávenite from the dyke border has higher Mg and Zn contents than wöhlerite from the dyke center (Table 2).

Other difference in EGM composition is related to the lower heavy REE contents of the EGMs at the dyke border than at the dyke center (Fig. 5). This seems to be a consequence of the crystallization of lávenite rather than of wöhlerite. Our data show that lávenite preferentially incorporates the heavy REE, whereas wöhlerite incorporates both the light and heavy REE (Fig. 5). The lávenite concomitant crystallization leads to a concurrence in the heavy REE partitioning between EGMs and lávenite.

CONCLUSIONS

The studied EGMs from Monte de Trigo reveal characteristics of their crystallization environment, i.e., magma composition

and concomitant crystallizing phases. The EGMs are characterized by moderate variations in Fe and Mn at the *M(2)* site

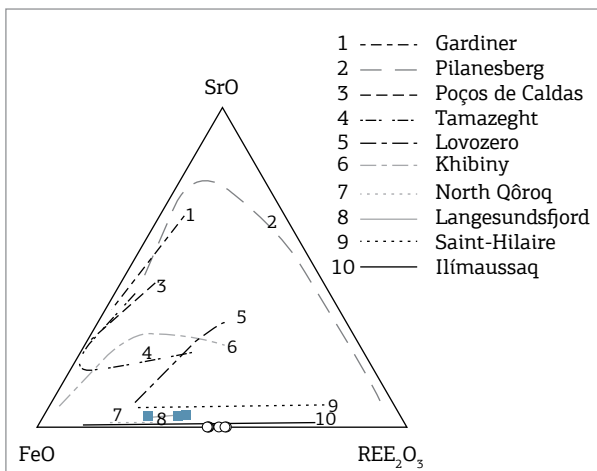


Figure 7. Ternary plot of FeO - SrO - REE_2O_3 for the EGMs from Monte de Trigo. Trend lines of the worldwide EGM compositions are compiled from Coulson & Chambers (1996), Gualda & Vlach (1996), Coulson (1997), Johnsen & Gault (1997), Olivio & Williams-Jones (1999), Johnsen & Grice (1999), Mitchell & Liferovich (2006), Marks et al. (2008), Schilling et al. (2009, 2011b), and Wu et al. (2010). Blue squares, the EGMs from the dyke border; open circles, the EGMs from the dyke center.

and Si and Nb at the *M(3,4)* site, which are recognized as the major substitution of EGMs worldwide. The relatively Na-poor, Ca-rich EGM compositions seem to be related to the Monte de Trigo transitional agpaitic rocks association, which contain wöhlerite and lävenite, and thus follow an agpaitic fluorine-rich trend. The low-Ba, Sr, and Eu contents are related to previous plagioclase fractionation during magmatic evolution and support the interpretation of a basanite parental magma for the suite. The incorporation and reaction of melatheralite xenoliths into the agpaitic magma could lead to higher Fe, Sr, Mg, and Zn contents in the EGMs found near the dyke border. Finally, the relative depletion of heavy REE in the EGMs from the dyke border seems to be related to the presence of lävenite, which strongly partitions heavy REE.

ACKNOWLEDGMENTS

The authors are grateful to Research Support Foundation of the State of São Paulo (FAPESP) (GERE, Processes 00/12576-4 and 2010/20476-1; CBG, Process 2013/18073-4; ER, Process 2012/06082-6) for financial support. The authors also thank Sandra Andrade and Marcos Mansueto for their assistance during the analytical work. Contributions by anonymous reviewers have significantly improved the manuscript.

REFERENCES

- Almeida F.F.M. 1983. Relações tectônicas das rochas alcalinas mesozóicas da região meridional da plataforma sul-americana. *Revista Brasileira de Geociências*, **13**(3):39-158.
- Andersen T., Erambert M., Larsen A.O., Selbekk R.S. 2010. Petrology of nepheline syenite pegmatites in the Oslo Rift, Norway: zirconium silicate mineral assemblages as indicators of alkalinity and volatile fugacity in mildly agpaitic magma. *Journal of Petrology*, **51**(11):2303-2325. DOI: 10.1093/petrology/egg058
- Azzone R.G., Ruberti E., Enrich G.E.R., Gomes C.B. 2009. Geologia e geocronologia do maciço alcalino máfico-ultramáfico Ponte Nova (SP-MG). *Geologia USP Série Científica*, **9**(2):23-46. DOI: <http://dx.doi.org/10.5327/z1519-874x2009000200002>
- Bailey J.C., Gwozdz R., Rose-Hansen J., Sørensen H. 2001. Geochemical overview of the Ilímaussaq alkaline complex, South Greenland. *Geology of Greenland Survey Bulletin*, **190**(100):35-53.
- Bastin G.F., Van Loo F.J.J., Heijligers H.J.M. 1984. Evaluation and use of gaussian Φ (pz) curves in quantitative electron probe microanalysis: a new optimization. *X-Ray Spectrometry*, **13**(2):91-97.
- Bédard J.H. 2006. Trace element partitioning in plagioclase feldspar. *Geochimica et Cosmochimica Acta*, **70**(14):3717-3742. DOI: 10.1016/j.gca.2006.05.003
- Blundy J.D. & Wood B.J. 1991. Crystal-chemical controls on the partitioning of Sr and Ba between plagioclase feldspar, silicate melts, and hydrothermal solutions. *Geochimica et Cosmochimica Acta*, **55**(1):193-209. DOI: 10.1016/0016-7037(91)90411-W
- Bollingberg H.J., Ure A.M., Sørensen I., Leonardsen E.S. 1983. Geochemistry of some eudialyte-eucolite troimens and a co-existing catapleiite from Langesund, Norway. *Tschermaks Mineralogische und Petrographische Mitteilungen*, **32**:153-169.
- Brotzu P., Barbieri M., Beccaluva L., Garbarino C., Gomes C.B., Macciotta G., Melluso L., Morbidelli L., Ruberti E., Sígolo J.B., Traversa G. 1992. Petrology and geochemistry of the Passa Quatro alkaline complex, Southeastern Brazil. *Journal of South American Earth Science*, **6**(4):237-252. DOI: 10.1016/0895-9811(92)90044-Y
- Brotzu P., Gomes C.B., Melluso L., Morbidelli L., Morra V., Ruberti E. 1997. Petrogenesis of coexisting SiO_2 -undersaturated to SiO_2 -oversaturated felsic igneous rocks: The alkaline complex of Itatiaia, southeastern Brazil. *Lithos*, **40**(2-4):133-156. DOI: 10.1016/S0024-4937(97)00007-8
- Brotzu P., Melluso L., Bennio L., Gomes C.B., Lustrino M., Morbidelli L., Morra V., Ruberti E., Tassinari C., D'Antonio M. 2007. Petrogenesis of the Early Cenozoic potassio alkaline complex of Morro de São João, southeastern Brazil. *Journal of South American Earth Science*, **24**(1):93-115. DOI: 10.1016/j.jsames.2007.02.006
- Brotzu P., Melluso L., D'Amelio F., Lustrino M. 2005. Potassic dykes and intrusions of the Serra do Mar Igneous Province (SE Brazil) In: Comin-Chiaromonti P. & Gomes C.B. (eds.) *Mesozoic to Cenozoic alkaline magmatism in the Brazilian Platform*. São Paulo, Edusp/FAPESP, p. 443-472.
- Bulakh A.G. & Petrov T.G. 2004. Chemical variability of eudialyte-group minerals and their sorting. *Neues Jahrbuch für Mineralogie Monatshefte*, **2004**:127-144. DOI: 10.1127/0028-3649/2004/0127

- Carbonin S., Liziero F., Fuso C. 2005. Mineral chemistry of accessory minerals in alkaline complexes from the Alto Paraguay Province In: Comin-Chiaromonti P. & Gomes C.B. (eds.) *Mesozoic to Cenozoic alkaline magmatism in the Brazilian Platform*. São Paulo, Edusp/FAPESP, p. 149-158.
- Carvalho B.B. & Janasi V.A. 2012. Crystallization conditions and controls on trace element residence in the main minerals from the Pedra Branca syenite, Brazil: an electron microprobe and LA-ICPMS study. *Lithos*, **153**(6):208-223.
- Chakhmouradian A.R., Mitchell R.H., Burns P.C., Mikhailova Y., Regur E.P. 2008. Marianoite, a new member of the cuspidine group from the Prairie Lake silicocarbonatite, Ontario. *The Canadian Mineralogist*, **46**(4):1023-1032. DOI: 10.3749/canmin.46.4.1023
- Chukanov N.V., Rastsvetaeva R.K., Rozenberg K.A., Aksenov S.M., Pekov I.V., Belakovskiy D.I., Kristiansen R. 2015. Ilyukhinite, IMA 2015-065. CNMNC Newsletter No. 28, December 2015, page 1860; *Mineralogical Magazine*, **79**(6):1859-1864. DOI: 10.1180/minmag.2015.079.7.18
- Comin-Chiaromonti P. & Gomes C.B. 2005. *Mesozoic to Cenozoic alkaline magmatism in the Brazilian Platform*. São Paulo, Edusp/FAPESP, 752 p.
- Coulson I.A. 1997. Post-magmatic alteration in eudialyte from the North Qôroq centre, South Greenland. *Mineralogical Magazine*, **61**:99-109. DOI: 10.1180/minmag.1997.061.404.10
- Coulson I.A. & Chambers A.D. 1996. Patterns of zonation in rare-earth-bearing minerals in nepheline syenites of the North Qôroq center, South Greenland. *The Canadian Mineralogist*, **34**:1163-1178.
- Deer W.A., Howie R.A., Zussman J. 1986. *Rock-forming minerals, volume 1B: Disilicates and Ring Silicates*. Oxford, The Geological Society Publishing House, 629 p.
- Enrich G.E.R., Azzone R.G., Ruberti E., Gomes C.B., Comin-Chiaromonti P. 2005. Itatiaia, Passa Quatro and São Sebastião Island, the major alkaline syenitic complexes from the Serra do Mar region In: Comin-Chiaromonti P. & Gomes C.B. (eds.) *Mesozoic to Cenozoic alkaline magmatism in the Brazilian Platform*. São Paulo, Edusp/FAPESP, p. 419-442.
- Enrich G.E.R., Ruberti E., Gomes C.B. 2009. Geology and geochronology of Monte de Trigo Island alkaline suite, southeastern Brazil. *Revista Brasileira de Geociências*, **39**(1):67-80.
- Gomes C.B., Laurenzi M.A., Censi P., De Min A., Velázquez V.F., Comin-Chiaromonti P. 1996. Alkaline magmatism from northern Paraguay (Alto Paraguay): a Permo-Triassic province In: Comin-Chiaromonti P. & Gomes C.B. (eds.) *Alkaline Magmatism in Central-Eastern Paraguay. Relationships with Coeval Magmatism in Brazil*. São Paulo, Edusp/Fapesp, p. 223-230.
- Grice J.D., Gault R.A. 2006. Johnsenite-(Ce): a new member of the eudialyte group from Mont Saint-Hilaire, Quebec, Canada. *The Canadian Mineralogist*, **44**(1):105-115. DOI: 10.2113/gscanmin.44.1.105
- Gualda G.A.R. & Vlach S.R.F. 1996. Eudialita-eucolita do maciço alcalino de Poços de Caldas, MG-SP: químismo e correlação com o comportamento ótico. In: 39º Congresso Brasileiro de Geologia, Anais, v. 3, p. 34-36.
- Henderson C.M.B. & Pierozynski W.J. 2012. An experimental study of Sr, Ba and Rb partitioning between alkali feldspar and silicate liquid in the system nepheline-kalsilite-quartz at 0.1 GPa P(H₂O): a revisit and reassessment. *Mineralogical Magazine*, **76**(1):157-190. DOI: 10.1180/minmag.2012.076.1.157
- Johnsen O. & Gault R.A. 1997. Chemical variation in eudialyte. *Neues Jahrbuch für Mineralogie-Abhandlungen*, **171**:215-237.
- Johnsen O. & Grice J.D. 1999. The crystal chemistry of the eudialyte group. *The Canadian Mineralogist*, **37**:865-891.
- Johnsen O., Ferraris G., Gault R.A., Grice J.D., Kampf A.R., Pekov I.V. 2003. The nomenclature of eudialyte-group minerals. *The Canadian Mineralogist*, **41**:785-794. DOI: 10.2113/gscanmin.41.3.785
- Johnsen O., Grice J.D., Gault R.A. 1998. Kentbrooksite from the Kangerdlugssuaq intrusion, East Greenland, a new Mn-REE-Nb-F end-member in a series within the eudialyte group: description and crystal structure. *European Journal of Mineralogy*, **10**(2):207-219. DOI: 10.1127/ejm/10/2/0207
- Johnsen O., Grice J.D., Gault R.A. 2001. The eudialyte group: a review. *Geology of Greenland Survey Bulletin*, **190**:65-72.
- Khomyakov A.P. 1995. *Mineralogy of hiperagpaitic rocks*. Oxford, Oxford Scientific Publications, Clarendon Press, 223 p.
- Khomyakov A.P., Dusmatov V.D., Ferraris G., Gula A., Ivaldi G., Nechelyustov G.N. 2003. Zirsilit-(Ce), (Na, \square)₁₂-(CeNa)₃Ca₆Mn₃Zr₃Nb(Si₂₅O₇₃)(OH)₃(CO₃)H₂O, and carbokentbrooksite (Na, \square)₁₂(Na,Ce)₃Ca₆Mn₃Zr₃Nb(Si₂₅O₇₃)(OH)₃(CO₃)H₂O: two new eudialyte-group minerals from the Dara-i-Pioz alkaline massif, Tajikistan. *Zapiski Vserossijskogo Mineralogicheskogo Obshchestva*, **132**:40-51.
- Khomyakov A.P., Nechelyustov G.N., Ekimenkova I.A., Rastsvetaeva R.K. 2005. Georgbarsanovite, Na₁₂(Mn,Sr,REE)₃Ca₆Fe²⁺₃Zr₃NbSi₂₅O₇₆Cl₂H₂O a mineral species of the eudialyte group: revalidation of barsanovite and the new name of the mineral. *Zapiski Rossijskogo Mineralogicheskogo Obshchestva*, **134**:47-57.
- Khomyakov A.P., Nechelyustov G.N., Rastsvetaeva R.K., Rozenberg K.A. 2008. Andrianovite, Na₁₂(K,Sr,Ce)₃Ca₆Mn₃Zr₃Nb(Si₂₅O₇₃)(O,H₂O,OH)₅, a new potassium-rich mineral species of the eudialyte group from the Khibiny alkaline Pluton, Kola Peninsula, Russia. *Geology of Ore Deposits*, **50**(8):705-712. DOI: 10.1134/S1075701508080060
- Kogarko L.N., Lahaye Y., Brey G.P. 2010. Plume-related mantle source of super-large rare metal deposits from the Lovozero and Khibina massifs on the Kola Peninsula, Eastern part of Baltic Shield: Sr, Nd and Hf isotope systematics. *Mineralogy and Petrology*, **98**(1):197-208. DOI: 10.1007/s00710-009-0066-1
- Kramm U. & Kogarko L.N. 1994. Nd and Sr isotope signatures of the Khibina and Lovozero agpaitic centres, Kola Alkaline Province, Russia. *Lithos*, **32**(3):225-242. DOI: 10.1016/0024-4937(94)90041-8
- Larsen L.M. & Sørensen H. 1987. The Ilímaussaq intrusion-progressive crystallization and formation of layering in an agpaitic magma In: Fitton J.G. & Upton B.G.J. (eds.) *Alkaline Igneous Rocks*. Geological Society Special Publications, 30, London, Geological Society of London, p. 473-488.
- Le Maitre R.W. (Ed.) 2002. *Igneous rocks: a classification of igneous rocks and glossary of terms*. Cambridge, Cambridge University Press, 236 p.
- Marks M.A.W., Hettmann K., Schilling J., Frost B.R., Markl G. 2011. The mineralogical diversity of alkaline igneous rocks: critical factors for the transition from miaskitic to agpaitic phase assemblages. *Journal of Petrology*, **52**(3):439-455. DOI: 10.1093/petrology/eqg086
- Marks M.A.W., Schilling J., Coulson I.M., Wenzel T., Markl G. 2008. The Alkaline-Peralkaline Tamazeght Complex, High Atlas Mountains, Morocco: mineral chemistry and petrological constraints for derivation from a compositionally heterogeneous mantle source. *Journal of Petrology*, **49**(6):1097-1131. DOI: 10.1093/petrology/egn019
- McDonough W. & Sun S.S. 1995. The composition of the Earth. *Chemical Geology*, **120**(3-4):223-253. DOI: 10.1016/0009-2541(94)00140-4
- Mellini M. 1981. Refinement of the crystal structure of låvenite. *Tschermaks Mineralogische und Petrographische Mitteilungen*, **28**:99-112. DOI: 10.1007/BF01081548
- Mellini M. & Merlini S. 1979. Refinement of the crystal structure of Wöhlerite. *Tschermaks Mineralogische und Petrographische Mitteilungen*, **26**(1):109-123. DOI: 10.1007/BF01081296

- Merlino S. & Perchiazzi N. 1988. Modular mineralogy in the cuspidine group of minerals. *The Canadian Mineralogist*, **26**(4):933-943.
- Mitchell R. & Liferovich R. 2006. Subsolidus deuteric/hydrothermal alteration of eudialyte in lujavrite from the Pilanesberg alkaline complex, South Africa. *Lithos*, **91**(1-4):352-372. DOI: 10.1016/j.lithos.2006.03.025
- Mitchell R.H. & Chakrabarty A. 2012. Paragenesis and decomposition assemblage of a Mn-rich eudialyte from the Sushina peralkaline nepheline syenite gneiss, Paschim Banga, India. *Lithos*, **152**:218-226. DOI: 10.1016/j.lithos.2012.02.003
- Morbidelli L., Gomes C.B., Beccaluva L., Brotzu P., Conte A.M., Ruberti E., Traversa G. 1995. Mineralogical, petrological and geochemical aspects of alkaline and alkaline-carbonatite associations from Brazil. *Earth-Science Reviews*, **39**(3):135-168. DOI: 10.1016/0012-8252(95)00031-3
- Mori P.E., Reeves S., Correia C.T., Haukka M. 1999. Development of a fused glass disc XRF facility and comparison with the pressed powder pellet technique at Instituto de Geociências, São Paulo University. *Revista Brasileira de Geociências*, **29**:441-446.
- Navarro M.S., Andrade S., Ulbrich H.H.G.J., Gomes C.B., Girardi V.A.V. 2008. The direct determination of rare earth elements in basaltic and related rocks using ICP-MS: testing the efficiency of microwave oven sample decomposition procedures. *Geostandards and Geoanalytical Research*, **32**(2):167-180. DOI: 10.1111/j.1751-908X.2008.00840.x
- Nielsen T.F.D. 1980. The petrology of a melilitolite, melteigite, carbonatite and syenite ring dike system, in the Gardiner complex, East Greenland. *Lithos*, **13**(2):181-197. DOI: 10.1016/0024-4937(80)90019-5
- Nomura S.F., Atêncio D., Chukanov N.V., Rastsvetaeva R.K., Coutinho J.M.V., Karipidis T.K. 2010. Manganoeudialyte: a new mineral from Poços de Caldas, Minas Gerais, Brazil. *Zapiski Rossiiskogo Mineralogicheskogo Obshchestva*, **38**:35-47.
- Olivo G.R. & Williams-Jones A.E. 1999. Hydrothermal REE-rich eudialyte from the Pilanesberg Complex, South Africa. *The Canadian Mineralogist*, **37**(3):653-663.
- Peate D.W. 1997. The Paraná-Etendeka Province In: Mahoney J.J. & Coffin M.F. (eds.) *Large Igneous Provinces*. Geophysical Monograph 100. Washington, American Geophysical Union, p. 217-245.
- Pekov I.V., Ekimenkova I.A., Chukanov N.V., Rastsvetaeva R.K., Kononkova N.N., Pekova N.A., Zadov A.E. 2001. Feklichevite $\text{Na}_{11}\text{Ca}_9(\text{Fe}^{3+},\text{Fe}^{2+})_2\text{Zr}_3\text{Nb}[\text{Si}_{25}\text{O}_{75}]_{2}[(\text{OH},\text{H}_2\text{O},\text{Cl},\text{O})_5]$, a new mineral of the eudialyte group from Kovdor Massif, Kola peninsula. *Zapiski Vserossijskogo Mineralogicheskogo Obshchestva*, **130**:55-65.
- Rastsvetaeva R.K. 2007. Structural mineralogy of the eudialyte group: a review. *Crystallography Reports*, **52**(1):47-64. DOI: 10.1134/S1063774507010063
- Rastsvetaeva R.K. & Chukanov N.V. 2012. Classification of eudialyte-group minerals. *Geology of Ore Deposits*, **54**(7):487-497. DOI: 10.1134/S1075701512070069
- Riccomini C., Velázquez V.F., Gomes C.B. 2005. Tectonic controls of the Mesozoic and Cenozoic alkaline magmatism in Central-Southeastern Brazilian Platform In: Comin-Chiaromonti P. & Gomes C.B. (eds.) *Mesozoic to Cenozoic alkaline magmatism in the Brazilian Platform*. São Paulo, Edusp/FAPESP, p. 31-55.
- Ridolfi F., Renzulli A., Macdonald R., Upton B.G.J. 2006. Peralkaline syenite autoliths from Kilombe volcano, Kenya Rift Valley: evidence for subvolcanic interaction with carbonatitic fluids. *Lithos*, **91**(1-4):373-392. DOI: 10.1016/j.lithos.2006.03.026
- Ridolfi F., Renzulli A., Santi P., Upton B.G.J. 2003. Evolutionary stages of crystallization of weakly peralkaline syenites: evidence from ejecta in the plinian deposits of Agua de Pau volcano (São Miguel, Azores Islands). *Mineralogical Magazine*, **67**(4):749-767. DOI: 10.1180/0026461036740131
- Schilling J., Marks M., Wenzel T., Markl G. 2009. Reconstruction of magmatic to subsolidus processes in an agpaitic system using eudialyte textures and composition: a case study from Tamazeght, Morocco. *The Canadian Mineralogist*, **47**(2):351-365. DOI: 10.3749/canmin.47.2.351
- Schilling J., Marks M.A.W., Wenzel T., Vennemann T., Horváth L., Tarassoff P., Jacob D.E., Markl G. 2011a. The magmatic to hydrothermal evolution of the intrusive Mont Saint-Hilaire Complex: insights into the late-stage evolution of peralkaline rocks. *Journal of Petrology*, **52**(11):2147-2185. DOI: 10.1093/petrology/egr042
- Schilling J., Wu F.-Y., McCammon C., Wenzel T., Marks M.A.W., Pfaff K., Jacob D.E., Markl G. 2011b. The compositional variability of eudialyte-group minerals. *Mineralogical Magazine*, **75**(1):87-115. DOI: 10.1180/minmag.2011.075.1.87
- Shannon R.D. 1976. Revised effective ionic radii and systematic studies of interatomic distances in halides and chalcogenides. *Acta Crystallographica Section A*, **32**:751-767. DOI: 10.1107/S0567739476001551
- Sørensen H. 1997. The agpaitic rocks, an overview. *Mineralogical Magazine*, **61**(4):485-498.
- Stromeyer F. 1819. Summary of meeting 16 December 1819. *Göttingische gelehrte Anzeigen*, **3**:1993-2000.
- Thompson R.N., Gibson S.A., Mitchell J.G., Dickin A.P., Leonardos O.H., Brod J.A., Greenwood J.C. 1998. Migrating Cretaceous-Eocene magmatism in the Serra do Mar Alkaline Province, SE Brasil: melts from the deflected Trindade Mantle Plume? *Journal of Petrology*, **39**(8):1493-1526. DOI: 10.1093/petroj/39.8.1493
- Ulbrich H.H.G.J. & Ulbrich M.N.C. 2000. The lujavrite and khibinite bodies in the Poços de Caldas alkaline massif, southeastern Brazil: a structural and petrographic study. *Revista Brasileira de Geociências*, **30**(4):615-622.
- Ulbrich H.H.G.J., Demaiffe D., Vlach S.R.F., Ulbrich M.N.C. 2005. Structure and origin of the Poços de Caldas alkaline massif, SE Brazil In: Comin-Chiaromonti P. & Gomes C.B. (eds.) *Mesozoic to Cenozoic alkaline magmatism in the Brazilian Platform*. São Paulo, Edusp/FAPESP, p. 367-418.
- Van Achterbergh E., Ryan C.G., Jackson S.E., Griffin W.L. 2001. Data reduction software for LA-ICP-MS: appendix In: Silvester P.J. (ed.) *Laser Ablation-ICP-Mass spectrometry in the Earth sciences: principles and applications*. Mineralogical Association of Canada Short Course Series 29, Ottawa, Mineralogical Association of Canada, p. 239-243.
- Williams C.T. 1996. Analysis of rare earth minerals In: Jones A.P., Wall F., Williams C.T. (eds.) *Rare earth minerals: chemistry, origin and ore deposits*. Mineralogical Society Series 7, London, Chapman & Hall, p. 327-348.
- Wu F.-Y., Yang Y.-H., Marks M.A.W., Liu Z.-C., Zhou Q., Ge W.-C., Yang J.-S., Zhao Z.-S., Mitchell R.H., Markl G. 2010. In situ U-Pb, Nd and Hf isotopic analysis of eudialyte by LA-(MC)-ICP-MS. *Chemical Geology*, **273**(1-2):8-34. DOI: <http://dx.doi.org/10.1016/j.chemgeo.2010.02.007>

Available at www.sbggeo.org.br